Condensed Matter Physics, 2013, Vol. 16, No 1, 13604: 1–14
DOI: 10.5488/CMP.16.13604
http://www.icmp.lviv.ua/journal

Adatom interaction effects in surface diffusion

Yu.B. Gaididei[1], V.M. Loktev[1], A.G. Naumovets[2], A.G. Zagorodny[1]

[1] Bogolyubov Institute for Theoretical Physics of the National Academy of Sciences of Ukraine, 14 b Metrologichna St., 03680 Kiev, Ukraine

[2] Institute of Physics of the National Academy of Sciences of Ukraine, 46 Nauki ave., 03680 Kiev, Ukraine

Received July 24, 2012, in final form October 3, 2012

Motivated by recent research of Nikitin et al. [J. Phys. D: Appl. Phys., 2009, **49**, 055301], we examine the effects of interatomic interactions on adatom surface diffusion. By using a mean-field approach in the random walk problem, we derive a nonlinear diffusion equation and analyze its solutions. The results of our analysis are in good agreement with direct numerical simulations of the corresponding discrete model. It is shown that by analyzing a time dependence of adatom concentration profiles one can estimate the type and strength of interatomic interactions.

Key words: *adatom, surface, nonlinear diffusion, numerical simulations*

PACS: *68.43.Jk, 68.35.Fx*

1. Introduction

Diffusion is ubiquitous in Nature. It determines the behavior and controls the efficiency of many biological and technological processes. Examples include the wetting, conductivity of biological membranes, catalysis, growth of crystals, sintering, soldering, etc. Surface diffusion is particularly important in nanotechnological processes which are aimed at obtaining objects of submicron sizes where the surface properties are of the same importance as the bulk ones. Macroscopic description of diffusion is based on Fick's law, which postulates proportionality between particle flux and concentration gradient. Establishing a link between macroscopic laws of diffusion and microscopic non-equilibrium density matrix approach is one of the most challenging and important problems of non-equilibrium statistical mechanics (for reviews see, e.g. [1–6]). Surface diffusion is essentially a many-particle process. Even at very low coverage when the interaction between adatoms is negligible, the random walk of an isolated adsorbed particle is a collective motion due its interaction with substrate atoms [4, 5]. The walker moves in a potential landscape which is changed by the walker [7]. The walk on a deformable medium where the walker leaves behind a trail and the trail affects the next walker due to slow relaxation, is also a collective process [8, 9]. At finite coverage, in addition to the interaction with a substrate, particles at surfaces experience lateral interactions of different origin: the attractive van der Waals, direct and indirect electronic exchange and multipole-multipole electrostatic interactions. The dipole-dipole interaction which occurs due to a polar (mainly dipolar) character of adsorption bonds is long-ranged (as r^{-3}) and generally repulsive since all dipole moments are essentially parallel (see review papers, e.g., [4, 5]).

Bowker and King [10] used Monte-Carlo simulations in order to clarify the effect of lateral interactions of adatoms on the shape of the evolving concentration profiles in surface diffusion. They showed that the intersection point of the diffusion profiles with the initial stepwise profile lies above $\theta_{\max}/2$ in the case of lateral repulsion and below $\theta_{\max}/2$ in the case of attraction ($\theta_{\max}$ is the maximum concentration at the initial step).

In a quite recent paper [11] an approach based on error function expansion was proposed to fit experimental concentration profiles. This algorithm provides a high-accuracy fitting and improves the accuracy of the concentration dependence of diffusivity extracted from experimental data. The goal of our paper is to model and examine the effects of interatomic interactions on adatom surface diffusion. Starting with nonlinear random walk equations where the interatomic interactions are considered in the mean-field approach, we derive a nonlinear diffusion equation and analyze its solutions. The results of our analysis are in good agreement with direct numerical simulations of the corresponding discrete model. It is shown that by analyzing a time dependence of adatom concentration profiles one can estimate the type and strength of interatomic interactions. The paper is organized as follows. In section 1 we present the model. In section 2 we study both analytically and numerically the interaction effects for the case of low adatom coverage. Section 3 is devoted to analytical treatment of nonlinear diffusion in the case of non-monotonous concentration dependence of the diffusion coefficient. We also compare our results with the results of full scale numerical simulations and the results of experimental observations. Section 4 presents some concluding remarks.

2. Model and equations of motion

The transport of particles on a surface is described by a set of random walk equations

$$\frac{\mathrm{d}}{\mathrm{d}t}\theta_{\vec{n}}(t) = \sum_{\vec{\rho}} \left\{W_{\vec{n}+\vec{\rho}\to\vec{n}}\,\theta_{\vec{n}+\vec{\rho}}(t)\left[1-\theta_{\vec{n}}(t)\right] - W_{\vec{n}\to\vec{n}+\vec{\rho}}\,\theta_{\vec{n}}(t)\left[1-\theta_{\vec{n}+\vec{\rho}}(t)\right]\right\}, \tag{2.1}$$

where $\theta_{\vec{n}}$ is the probability for a particle to occupy the $\vec{n}$-th binding site on the surface (in the literature on surface science, this quantity has the meaning of coverage), $W_{\vec{n}\to\vec{n}+\vec{\rho}}$ gives the rate of the jumps from the binding site $\vec{n}$ to a neighboring site $\vec{n}+\vec{\rho}$ (the vector $\vec{\rho}$ connects the nearest neighbors). The terms $[1-\theta_{\vec{n}}(t)]$ in equations (2.1) take into account the fact that there may be only one adatom at a given site or, in other words, the so-called kinematic interaction. The probability with which the particle jumps from site $\vec{n}$ to the nearest neighbor $\vec{n}+\vec{\rho}$ satisfies the detailed balance condition

$$W_{\vec{n}\to\vec{n}+\vec{\rho}}\,\mathrm{e}^{-\beta E_{\vec{n}}} = W_{\vec{n}+\vec{\rho}\to\vec{n}}\,\mathrm{e}^{-\beta E_{\vec{n}+\vec{\rho}}}, \tag{2.2}$$

where $E_{\vec{n}}$ is the binding energy of the particle located at site $\vec{n}$, $\beta = 1/k_{\mathrm{B}}T$, k_{B} is the Boltzmann constant and T is the temperature of the system. For transition rates we choose

$$W_{\vec{n}\to\vec{n}+\vec{\rho}} = w_{\vec{\rho}}\,\mathrm{e}^{\beta E_{\vec{n}}}, \tag{2.3}$$

which corresponds to setting the activation energy for a jump to the initial binding energy. Here, $w_{\vec{\rho}} = \nu_{\vec{\rho}}\,\mathrm{e}^{-\beta E_b}$ $\left(w_{\vec{\rho}} = w_{-\vec{\rho}}\right)$ is the jump rate of an isolated particle with standard notations: $\nu_{\vec{\rho}}$ is a frequency factor and $E_b - E_{\vec{n}}$ is the height of the random walk barrier. Inserting equation (2.3) into equations (2.1) we obtain a description of the random walk of particles on the surface by a set of equations

$$\frac{\mathrm{d}}{\mathrm{d}t}\theta_{\vec{n}}(t) = \sum_{\vec{\rho}} w_{\vec{\rho}} \left\{\left[1-\theta_{\vec{n}}(t)\right]\theta_{\vec{n}+\vec{\rho}}(t)\,\mathrm{e}^{\beta E_{\vec{n}+\vec{\rho}}} - \theta_{\vec{n}}(t)\left[1-\theta_{\vec{n}+\vec{\rho}}(t)\right]\mathrm{e}^{\beta E_{\vec{n}}}\right\}. \tag{2.4}$$

In the case when the characteristic size of the particle distribution inhomogeneity is much larger than the lattice spacing, one can replace $\theta_{\vec{n}}$ and $E_{\vec{n}}$ by the functions $\theta(\vec{r})$ and $E(\vec{r})$ of the continuous variable $\vec{r}$ and, by expanding the functions $\theta(\vec{r}+\vec{\rho})$ and $E(\vec{r}+\vec{\rho})$ into a Taylor series, we obtain from equations (2.4) a description of the transport of particles on the surface in the continuum approximation by the equation of the form

$$\partial_t\theta = w\vec{\nabla}\left\{\left[\vec{\nabla}\theta + \beta\theta\,(1-\theta)\,\vec{\nabla}E\right]\mathrm{e}^{\beta E}\right\}, \tag{2.5}$$

where the notation $w = \frac{1}{2}\sum_{\vec{\rho}}\vec{\rho}^{\,2}\,w_{\vec{\rho}}$ is used.

We will study the particle kinetics in the mean field approach when the binding energy E is assumed to be a functional of the particle density $\theta(\vec{r},t)$: $E(\vec{r}) = \mathscr{E}(\theta)$. Note that the passage through a saddle point which separates two neighboring binding sites is also sensitive to interparticle interactions. However, taking into consideration that a lion's share of time the particles dwell near the potential well minima, one can expect that the interaction more strongly effects the particle propagation by modifying the binding energy. In this case, equation (2.5) takes the form of nonlinear diffusion equation

$$\partial_t\theta = \vec{\nabla}\left[D(\theta)\,\vec{\nabla}\theta\right], \tag{2.6}$$

where

$$D(\theta) = w\left[1+\beta\theta\,(1-\theta)\,\frac{\delta\mathscr{E}}{\delta\theta}\right]\mathrm{e}^{\beta\mathscr{E}} \tag{2.7}$$

is a nonlinear (i.e., collective) diffusion coefficient.

3. Surface diffusion at low coverage

In what follows we restrict ourselves to studying the particle distributions spatially homogeneous along the y coordinate: $\theta(\vec{r},t)\equiv\theta(x,t)$. We assume that initially the particles are step-like distributed

$$\theta(x,0) = \theta_{\max}\,H(-x)\,, \tag{3.1}$$

where $H(x)$ is the Heaviside step function. By introducing a centered particle density $\xi(x,t) = [\theta(x,t)-0.5\theta_{\max}]\,/\theta_{\max}$, we see that the initial distribution $\xi(x,0)$ is an odd function of the spatial variable x. It is obvious that in the no-interaction case ($\mathscr{E}=\text{const}$), when the diffusion equation (2.6) is linear, the antisymmetric character of the function $\xi(x,t)$ is preserved for all $t>0$. This means that in the case of noninteracting particles, the concentration profile for each time moment t passes through the point $(0,\theta_{\max}/2)$. However, the interacting diffusing particles exhibit quite a different behavior. In 1969, Vedula and one of the present authors for the first time found out that the concentration profiles formed in the process of surface diffusion of thorium on tungsten intersected the initial step-like profile at a point lying well above $\theta_{\max}$ (see [2, 13]). Since then, similar behavior has been found for many electropositive adsorbates whose adatoms are known to interact repulsively. A recent example obtained in the case of surface diffusion of Li on the Dy-Mo (112) surface was discussed in [11]. It is worth noting that the above mentioned behavior was observed even for rather low coverage: $\theta_{\max}<0.3$ (see figure 2 in [11]). Therefore, to explain such a behavior one may assume that the binding energy $E(\vec{r})$ is linearly dependent on the particle concentration:

$$E(\vec{r}) = E_0 + \int \mathrm{d}\vec{r}\,'\,V(\vec{r}-\vec{r}\,')\,\theta(\vec{r}\,')\,, \tag{3.2}$$

where E_0 is the site energy and $V(\vec{r}-\vec{r}\,')$ is the effective adatom-adatom interaction which includes all types of lateral interactions. By using a Fourier representation of the interaction $V(\vec{r})$ and the particle density $\theta(\vec{r})$

$$V(\vec{r}) = \int \mathrm{d}\vec{r}\,\mathrm{e}^{\mathrm{i}\vec{k}\vec{r}}\,\hat{V}(\vec{k})\,, \qquad \theta(\vec{r}) = \int \mathrm{d}\vec{r}\,\mathrm{e}^{\mathrm{i}\vec{k}\vec{r}}\,\hat{\theta}(\vec{k})\,, \tag{3.3}$$

equation (3.2) can be written in the form

$$E(\vec{r}) = E_0 + \int \mathrm{d}\vec{k}\,\mathrm{e}^{\mathrm{i}\vec{k}\vec{r}}\,\hat{V}(\vec{k})\,\hat{\theta}(-\vec{k})\,. \tag{3.4}$$

By expanding the Fourier component of the interaction $V(\vec{r})$ into a Taylor series

$$\hat{V}(\vec{k}) = \hat{V}(0) + \frac{1}{2}\,\frac{\partial^2\hat{V}(\vec{k})}{\partial k_\alpha \partial k_\beta}\bigg|_{\vec{k}=0} k_\alpha\,k_\beta + \ldots \tag{3.5}$$

and using an inverse Fourier transform, one can represent the expression (3.2) as follows:

$$E(\vec{r}) - E_0 = \hat{V}(0)\theta(\vec{r}) - \frac{1}{2}\,\frac{\partial^2\hat{V}(\vec{k})}{\partial k_\alpha \partial k_\beta}\bigg|_{\vec{k}=0}\frac{\partial^2}{\partial\alpha\,\partial\beta}\,\theta(\vec{r}). \tag{3.6}$$

In equations (3.5) and (3.6) $\alpha, \beta = x, y$ and Einstein's summation rule is applied. The first term in the right-hand side of equation (3.6) characterizes the change of the energy barrier due to the finite concentration of adatoms on the surface (i.e., mean field approximation) and the second one represents dispersion effects. In what follows we restrict ourselves to the mean field approximation. This implies the assumption that the binding energy $E(\vec{r})$ is expressed as follows:

$$E(\vec{r}) = E_0 + \theta(\vec{r}) \int \mathrm{d}\vec{r}'\, V(\vec{r}') \tag{3.7}$$

and the nonlinear diffusion coefficient (2.7) takes the form

$$D(\theta) = D^* \left[1 + \alpha\,\theta\,(1-\theta)\right] \mathrm{e}^{\alpha\theta}\,, \tag{3.8}$$

where

$$D^* = w\,\mathrm{e}^{\beta E_0} \equiv \nu\,\mathrm{e}^{-\beta\,(E_b - E_0)} \tag{3.9}$$

is the diffusion coefficient for an isolated particle (or the so-called tracer diffusion coefficient) and the dimensionless parameter

$$\alpha \equiv \beta V_0\,, \qquad V_0 = \int \mathrm{d}\vec{r}'\, V(\vec{r}')$$

characterizes the strength of the lateral interaction.

Diffusion equations with concentration-dependent diffusion coefficients are widely explored in literature. A vast variety of tools which permit to study nonlinear diffusion processes both analytically and numerically are described in [12]. The goal of this section is to develop a new simple perturbation approach which permits to directly estimate the effects of interparticle interactions in the surface diffusion.

It is seen from equations (2.6) that the spatio-temporal behavior of the centered particle density $\xi(x,t)$ is governed by the equation

$$\partial_\tau \xi = \partial_x^2 \left[\xi + P(\xi)\right], \tag{3.10}$$

where $\tau = D_0\, t$ is a rescaled time and the quantity

$$P(\xi) = \frac{1}{D^*} \int\limits_0^{(1/2+\xi)\theta_{\max}} D(\theta)\,\mathrm{d}\theta - \left(\frac{1}{2} + \xi\right)\theta_{\max} \tag{3.11}$$

describes the nonlinear properties of the diffusion and vanishes when $\alpha \to 0$. Taking into account that equation (3.10) with the initial condition given by equation (3.1) is invariant under gauge transformations $\tau \to \lambda^2 \tau$, $x \to \lambda\, x$, $\theta \to \theta$ (λ is an arbitrary number) one can look for a solution of equation (3.10) in terms of the Boltzmann variable

$$z = \frac{x}{2\sqrt{\tau}}\,, \qquad \xi(x,\tau) = \zeta(z)\,,$$

where the function $\zeta(z)$ satisfies the equation

$$\frac{\mathrm{d}^2}{\mathrm{d}z^2}\left[\zeta + P(\zeta)\right] + 2z\frac{\mathrm{d}\zeta}{\mathrm{d}z} = 0 \tag{3.12}$$

with the boundary conditions

$$\zeta(z) \to \mp\frac{1}{2}, \qquad z \to \pm\infty\,. \tag{3.13}$$

Equations (3.12), (3.13) can be rewritten in the form of the following integral equation:

$$\begin{aligned}
\zeta(z) &= \frac{\sqrt{\pi}}{4}\int\limits_0^\infty \mathrm{d}z\, w_+(z) - \frac{1}{2}\left[1 - \frac{\sqrt{\pi}}{2}\int\limits_0^\infty \mathrm{d}z\, w_-(z)\right]\mathrm{erf}(z) \\
&\quad - \frac{\sqrt{\pi}}{2}\int\limits_0^z \mathrm{d}z_1\, \mathrm{e}^{z_1^2}\left[\mathrm{erf}(z) - \mathrm{erf}(z_1)\right]\frac{\mathrm{d}^2}{\mathrm{d}z_1^2}P\big(\zeta(z_1)\big)\,, \\
w_\pm(z) &= \mathrm{e}^{z^2}\left[1 - \mathrm{erf}(z)\right]\frac{\mathrm{d}^2}{\mathrm{d}z^2}\left[P\big(\zeta(z)\big) \pm P\big(\zeta(-z)\big)\right],
\end{aligned} \tag{3.14}$$

where erf(z) is the error function [20]. It is seen from equation (3.14) that the concentration profiles $\xi(x,t)$ for different time moments intersect at the point $\big(0,\zeta(0)\big)$ with

$$\zeta(0) = \frac{\sqrt{\pi}}{4}\int\limits_0^\infty \mathrm{d}z\, w_+(z)\,. \tag{3.15}$$

In the weak interaction/low coverage limit when $\alpha\theta_{\max} < 1$ one can replace the function $\zeta(z)$ in the right-hand-side of equations (3.14), (3.15) by its expression obtained in the linear case: $\zeta_0(z) = \frac{1}{2}\,\mathrm{erf}(z)$ and state approximately that under the step-like initial condition (3.1) the concentration profiles $\theta(x,\tau)$ for different time moments intersect at the point which corresponds to the concentration

$$\begin{aligned}
\theta_0 &= \left[\frac{1}{2}+\zeta(0)\right]\theta_{\max}\,,\\
\zeta(0) &= \frac{\pi-2}{4\pi}\,\alpha\left(1-\frac{\theta_{\max}}{2}\right)\theta_{\max} \approx 0.091\,\alpha\left(1-\frac{\theta_{\max}}{2}\right)\theta_{\max}\,.
\end{aligned} \tag{3.16}$$

Thus, the concentration value θ_0 at which the concentration profiles intersect changes in the presence of lateral interatomic interactions: $\theta_0 > \theta_{\max}/2$ ($\theta_0 < \theta_{\max}/2$) when the interaction is repulsive (attractive). We used equation (3.16) to analyze the results obtained in [11] for the diffusion of Li on the Dy-Mo (112) surface at low coverage ($\theta_{\max} \approx 0.33$) for which $\theta_0 \approx 0.19$. First, we checked if our results which were obtained for an infinite domain can be applied for the samples used in experiments [11]. It is obvious that samples can be considered as physically infinite when the length of the sample L is large compared with the diffusion length:

$$L \gg \sqrt{D\, t_{\exp}}\,, \tag{3.17}$$

where $t_{\exp}$ is the time during which the experiment was performed. The parameters used in [11] are $D \sim 10^{-7} \div 10^{-9}$ cm^2/s, $t_{\exp} \sim 10^3$ s, $L \sim 10^{-1}$ cm. They clearly satisfy the inequality (3.17). Comparing experimental and our theoretical results we found out that $\alpha\theta_{\max} \approx 1$. It is seen that strictly speaking it is not fully legitimate to use our simple analytical perturbation approach (which is valid for $\alpha\theta_{\max} \ll 1$) to analyze the results of experiments [11] but a qualitative agreement takes place.

To validate our analytical results we have carried out numerical simulations of equations (2.4), (2.3) which in the 1D-case for a system with N binding sites have the form

$$\begin{aligned}
\frac{\mathrm{d}}{\mathrm{d}\tau}\theta_1 &= (1-\theta_1)\,\mathrm{e}^{\beta\mathscr{E}_2}\,\theta_2 - (1-\theta_2)\,\mathrm{e}^{\beta\mathscr{E}_1}\,\theta_1\,,\\
\frac{\mathrm{d}}{\mathrm{d}\tau}\theta_n &= (1-\theta_n)\left(\mathrm{e}^{\beta\mathscr{E}_{n+1}}\,\theta_{n+1}+\mathrm{e}^{\beta\mathscr{E}_{n-1}}\,\theta_{n-1}\right) - (2-\theta_{n+1}-\theta_{n-1})\,\mathrm{e}^{\beta\mathscr{E}_n}\,\theta_n, \qquad (n=2,\dots,N-1)\,,\\
\frac{\mathrm{d}}{\mathrm{d}\tau}\theta_N &= (1-\theta_N)\,\mathrm{e}^{\beta\mathscr{E}_{N-1}}\,\theta_{N-1} - (1-\theta_{N-1})\,\mathrm{e}^{\beta\mathscr{E}_N}\,\theta_N\,,
\end{aligned} \tag{3.18}$$

where $\beta\mathscr{E}_n = \alpha\theta_n$. Thus, in our model, the total number of particles is a conserved quantity. As an initial state we used a step-like distribution

$$\begin{aligned}
&\theta_n = \theta_{\max}\,, \qquad &&\text{for } 1 \leqslant n \leqslant N/2\,,\\
&\theta_n = 0\,, &&\text{otherwise}\,.
\end{aligned} \tag{3.19}$$

In figure 1, the intersection concentration θ_0 as a function of the interaction parameter α obtained at very low coverage ($\theta_{\max} = 0.1$) within the framework of the analytical approach [see equation (3.16)] is compared with the results of numerical simulations. It is seen that in the limit of weak interparticle interaction ($\alpha < 1$), the agreement is very good. The results of the numerical simulations obtained for the case of intermediate coverage are presented in figure 2. We found out that as in the experiment [11] for $\theta_{\max} = 0.33$ at early stages of evolution, the concentration profiles intersect at the point $(N/2, 0.186)$, i.e., well above the level $\theta_{\max}/2$ for $\alpha \approx (3 \div 3.5)$ (see figure 2, left-hand panel) or $\alpha\theta_{\max} \approx (1 \div 1.15)$ which is in a good agreement with our analytics. However, this intersection point shifts downward and to the

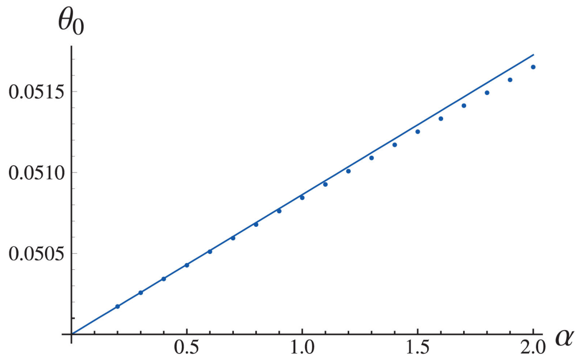

Figure 1. (Color online) Intersection concentration θ_0 as a function of the interaction parameter α obtained from numerical simulations (dots) and from equation (3.16) (solid line) for $\theta_{\max} = 0.1$.

right at the late stage of evolution (see figure 2, right-hand panel). Thus, basing on our approach one can conclude that Li adatoms on the Dy-Mo (112) surface mostly repel each other and the intensity of the repulsion is $V_0 \approx (3 \div 3.5)\, k_{\mathrm{B}}\, T$.

Diffusion of Li adatoms on Dy/Mo(112) was investigated experimentally at $T = 600$ K [11], so the estimated repulsion energy V_0 amounts to ≈ 0.16 eV. Let us assess this value in terms of the dipole-dipole interaction. The energy of the repulsive interaction between two dipoles having moments p and located on the surface at a distance r is

$$U_{\mathrm{dd}} = 2\,\frac{p^2}{r^3} \approx \frac{1.25\, p^2\,[\text{Debyes}]}{r^3\,[\text{Angstroms}]}\,[\text{eV}]\,. \tag{3.20}$$

The dipole moment can be determined from the work function change $\Delta\varphi$ using the Helmholtz formula for the double electric layer:

$$|\,\Delta\varphi\,| = 4\pi\, n_{\mathrm{a}}\, p\, e\,, \tag{3.21}$$

where n_{a} is the surface concentration of adatoms and e is the electronic charge. For Li on the Mo(112) surface, the p value at low coverage was found to be 1.4 Debyes [14]. Then, using equation (3.20) we can

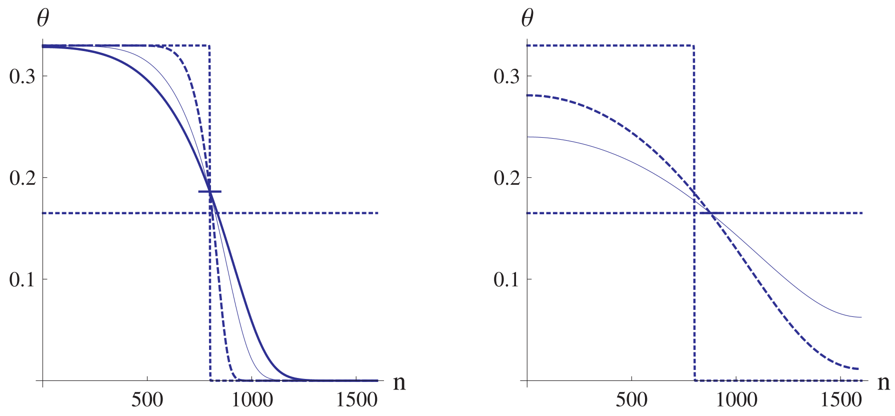

Figure 2. (Color online) Concentration profiles obtained from nonlinear random walk equations (3.18) for $\alpha = 3$ and initial distribution given by thin dashed curves. The left-hand panel shows an early stage of evolution: $wt = 1000$ (dashed curve), $wt = 5000$ (solid thin curve), $wt = 10000$ (thick solid curve); the right-hand panel shows the late stage of evolution: $wt = 50000$ (dashed), $wt = 100000$ (solid). The line which corresponds to $\theta = \theta_{\max}/2$ is shown as a horizontal dotted line. The point $n = N/2$, $\theta = 0.186$ where concentration profiles at the early stage of evolution intersect is marked as a line segment. In the same way, the intersection point at the late stage of the evolution is marked on the right-hand panel. The parameters used are $N = 1600$, $\alpha = 3$.

find that for two dipoles of this kind the interaction energy $U_{dd} = 0.16$ eV can be attained at a distance $r \approx 2.5$ Å, which is close to the distance between the nearest adsorption sites (2.73 Å) within the atomic troughs on Mo(112). This estimation shows that the intensity of the lateral interaction deduced from the diffusion data in the way presented above seems physically reasonable. Recall, however, that V_0 determines a resultant effect experienced by a jumping particle from all its counterparts which, in the case of heterodiffusion, are non-uniformly distributed over the surface and provide an additional driving force (supplementary to the coverage gradient) that favors a faster diffusion of repulsing particles.

4. Mean-square deviation

The adatom interactions also manifest themselves in the integral characteristics of kinetics of adatom diffusion. It is well known that in the linear regime the variance

$$\langle x^2\rangle = \int_{-\infty}^{\infty} \mathrm{d}x\, x^2\, \theta(x,\tau) \Big/ \int_{-\infty}^{\infty} \mathrm{d}x\, \theta(x,\tau) \tag{4.1}$$

behaves (in one-dimensional case) as $\langle x^2\rangle = 2\tau$. Therefore, it is only natural to introduce a variance rate

$$\Delta(\tau) = \left(2 - \frac{\mathrm{d}}{\mathrm{d}\tau}\langle x^2\rangle\right)^2 \tag{4.2}$$

whose time dependence provides a useful information on nonlinear effects in the diffusion process.

For this quantity, from equation (3.10) we obtain

$$\Delta(\tau) = \alpha^2 \left[\int_{-\infty}^{\infty} \mathrm{d}x\, \theta^2(x,\tau) \Big/ \int_{-\infty}^{\infty} \mathrm{d}x\, \theta(x,\tau)\right]^2 . \tag{4.3}$$

Assuming that initially the particles concentrate in a finite domain in a Π-like form:

$$\theta(x,0) = \theta_{\max}\Big(H(x+l) - H(x-l)\Big), \tag{4.4}$$

where $2l$ is the size of the initial domain, for small nonlinearities α and low coverage $\theta_{\max} \ll 1$ we approximately obtain

$$\Delta(\tau) = \alpha^2 \left[\int_{-\infty}^{\infty} \mathrm{d}x\, \theta^2_{\mathrm{lin}}(x,\tau) \Big/ \int_{-\infty}^{\infty} \mathrm{d}x\, \theta_{\mathrm{lin}}(x,\tau)\right]^2 , \tag{4.5}$$

where

$$\theta_{\mathrm{lin}}(x,\tau) = \frac{\theta_{\max}}{2}\left[\mathrm{erf}\left(\frac{l-x}{2\sqrt{\tau}}\right) - \mathrm{erf}\left(-\frac{l+x}{2\sqrt{\tau}}\right)\right] \tag{4.6}$$

is the solution of the linear diffusion equation with the initial condition (4.4). In the limit of small l we obtain

$$\Delta(\tau) \approx \frac{\alpha^2\theta^2_{\max}}{2\pi\tau}\, l^2 . \tag{4.7}$$

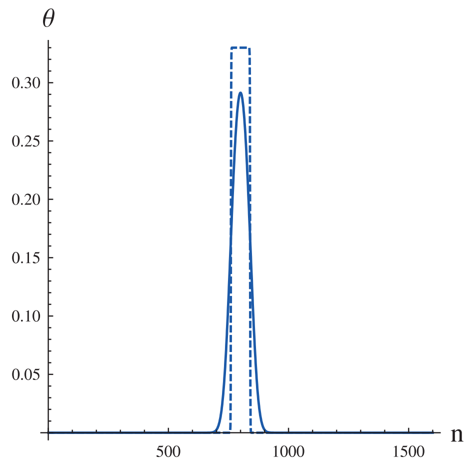

Figure 3. (Color online) Concentration profiles for initial pulse-like distribution (dashed line) and for $\tau = 200$ (solid line). The nonlinearity parameter $\alpha = 0.2$.

We checked our analytical considerations by carrying out numerical simulations of equations (3.18) with the initial concentration profile given by equation (4.4) (see figure 3) for different values of the nonlinearity parameter α. The results of these simulations are presented in figure 4. The figure shows that the numerically evaluated temporal behavior of the rate function Δ is in a good agreement with our analytical expression given by equation (4.7). Moreover, the slopes of the curves, as it is prescribed by the analytics, relate as $0.51 : 0.91 : 2.0 : 3.6 \approx \alpha_1^2 : \alpha_2^2 : \alpha_3^2 : \alpha_4^2 = 0.15^2 : 0.2^2 : 0.3^2 : 0.4^2$. Thus, by measuring the temporal behavior of concentration profiles, it is also possible to estimate the strength of interatomic interactions.

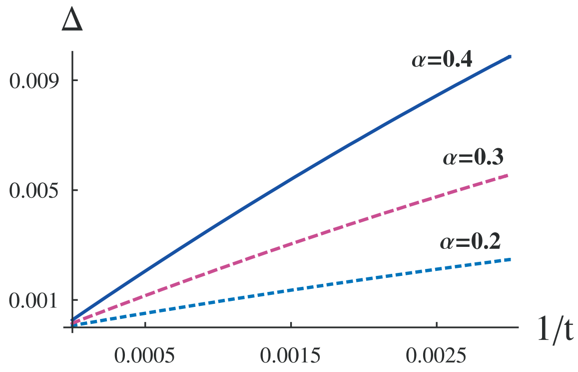

Figure 4. (Color online) Numerically obtained variance rate Δ given equation (4.2) as a function of the inverse time $1/t$ for three different values of the nonlinearity parameter α: $\alpha = 0.2$ (dotted line), $\alpha = 0.3$ (dashed line), $\alpha = 0.4$ (solid line).

5. Concentration profiles with plateau

In general, the diffusion coefficient is a non-monotonous function of atomic concentration (see e.g. [5]). There is a number of physical reasons which can cause a non-monotonous coverage dependence of the diffusion coefficient. It is well known that in thermodynamic terms, the diffusion flux is proportional to the gradient of chemical potential of adsorbed particles μ which can be written as [15, 16]

$$\mu = \mu_0 - q(\theta) + \frac{1}{\beta}\ln\left(\frac{\theta}{1-\theta}\right). \tag{5.1}$$

The first term in this equation is the standard chemical potential of the adsorbate, $q(\theta)$ is the differential heat of adsorption and the third term stems from the entropy of mixing of adatoms with the vacant adsorption sites on the substrate. (Note that this simplified expression relates only to the first monolayer and does not take into account the possibility of formation of the second and next monolayers). The diffusion coefficient can be represented as a product

$$D(\theta) = D_j\,\beta\left(\frac{\partial\mu}{\partial\ln\theta}\right), \tag{5.2}$$

where D_j is the so-called kinetic factor (or jump diffusion coefficient) [1, 5, 16] and the derivative in the brackets is referred to as thermodynamic factor. In the simplest case, when there are no cross-correlations between the velocities of diffusing particles, D_j coincides with the tracer diffusion coefficient D^* given by equation (3.9). Inserting equation (5.1) into equation (5.2), we get

$$D(\theta) = D_j\left(-\beta\theta\frac{\partial q}{\partial\theta} + \frac{1}{1-\theta}\right). \tag{5.3}$$

It is seen from equation (5.3) that any effect which entails a sharp decrease in the heat of adsorption as a function of coverage will result in a maximum of the diffusion coefficient in this coverage range [17]. For instance, such a situation occurs when all energetically profitable sites at the surface are occupied and adatoms start to fill less favorable sites. Actually, Bowker and King [10] found in their Monte Carlo simulations that a well-pronounced maximum in the $D(\theta)$ dependence observed by Butz and Wagner [21] can be explained by the existence of two types of lateral interactions: a repulsive one between the nearest neighbors and an attractive one between the next-nearest neighbors. A similar effect is typical of volume diffusion of interstitial atoms in disordered binary alloys having a BCC structure with two nonequivalent interstitial positions [22]. In the framework of local equilibrium statistical operator approach [23] it was shown that the physical reason for a non-monotonous concentration dependence coefficient is a combined action of lateral interaction and adatom density fluctuations [24]. A sharp drop in the heat of adsorption is also observed in the transition from filling the first, strongly bound (chemisorbed) monolayer to filling the second, weakly bound (e.g., physisorbed) monolayer. In such a case, the spreading of

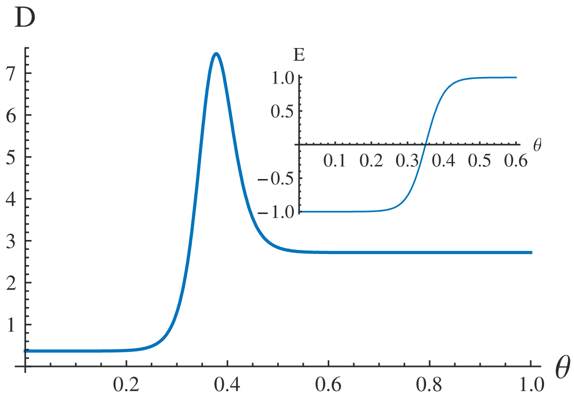

Figure 5. (Color online) Diffusion coefficient for a step-like on-site energy. The inset shows the concentration dependence of the on-site energy. The parameters used are $\alpha = 1$, $\kappa = 20$, $\theta_{\rm thr} = 0.5$.

the first monolayer proceeds through diffusion in the mobile uppermost (second or next) monolayer (the so-called "unrolling carpet" mechanism) [1]. This example shows that a change in the heat of adsorption can be accompanied not only by variation of the diffusion parameters (the activation energy and prefactor D_0 in the Arrhenius equation), but also by a change in the atomistic diffusion mechanism itself.

It is worth noting that without entering the microscopic mechanisms of the non-monotonous concentration diffusion coefficient dependence, it may be phenomenologically connected with a step-like dependence of the heat of adsorption on the coverage (see a review paper [25]). A typical example of the diffusion coefficient calculated from equation (2.7) by assuming the on-site adatom energy $\mathscr{E}(\theta)$ (which in most cases is proportional to the heat adsorption $q(\theta)$) has the form

$$\mathscr{E}(\theta) = \alpha\left[1 + \tanh\kappa\left(\theta - \theta_{\rm thr}\right)\right] \tag{5.4}$$

shown in figure 5. In equation (5.4) the parameter $\theta_{\rm thr}$ gives the threshold value of the coverage and the parameter κ characterizes the sharpness of the transition to the new state [26].

The aim of this section is to consider both analytically and numerically the diffusion process with a step-like concentration dependent on-site energy given by equation (5.4) and to clarify what kind of new information one can derive by comparing the theoretically obtained concentration profiles with the experimental ones.

It is very hard and probably hopeless to solve the equation (2.6) with the diffusion coefficient given by equations (2.7) and (5.4). However, the problem can be solved and some insight into the kinetics can be achieved in the limiting case of a very sharp energy concentration dependence: $\kappa \to \infty$. In this case, the diffusion coefficient (2.7) and (5.4) takes the form

$$D(\theta) = D^{*}\left[1 + a\,\delta\big(\theta - \theta_{\rm thr}\big) + b\,H\big(\theta - \theta_{\rm thr}\big)\right], \tag{5.5}$$

where

$$a = \alpha\,{\rm e}^{\alpha}\theta_{\rm thr}\left(1 - \theta_{\rm thr}\right), \qquad b = {\rm e}^{2\alpha} - 1. \tag{5.6}$$

The nonlinear diffusion equation (2.6) with the diffusion coefficient (5.5) and the initial condition (3.1) has a self-similar solution $\theta(x,\tau) \equiv \Theta(z)$, $(z = x/2\sqrt{\tau})$ which can be presented in the form (see appendix for a detailed derivation)

$$\theta(x,\tau) = \begin{cases} \theta_{\rm thr}\,\dfrac{{\rm erfc}\left(\frac{x}{2\sqrt{\tau}}\right)}{{\rm erfc}\,(z_1)}\,, & \text{when} \quad x \geqslant 2\,z_1\sqrt{\tau}\,, \\ \theta_{\rm thr}\,, & \text{when} \quad -2\,z_2\sqrt{\tau}\,{\rm e}^{\alpha} \leqslant x \leqslant 2\,z_1\sqrt{\tau}\,, \\ \theta_{\max} - \left(\theta_{\max} - \theta_{\rm thr}\right)\dfrac{{\rm erfc}\left(-\frac{x}{2\sqrt{\tau}}\,{\rm e}^{-\alpha}\right)}{{\rm erfc}\,(z_2)}\,, & \text{when} \quad x \leqslant -2\,z_2\,{\rm e}^{\alpha}\sqrt{\tau}\,. \end{cases}$$

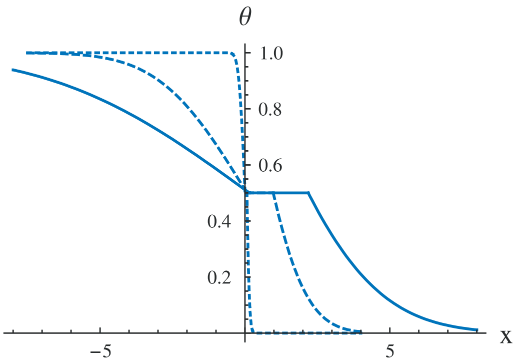

Figure 6. (Color online) Analytically obtained concentration profile for the diffusion coefficient in the δ-function limit (5.5) with $\alpha = 1$, $\theta_{\mathrm{thr}} = 0.5$, $\Theta_{\max} = 1$ for three different time moments: $\tau = 0.005$ (dotted line), $\tau = 1$ (dashed line), $\tau = 5$ (solid line).

Here, the parameters z_1 and z_2 are determined by the equations

$$\begin{aligned} z_2 &= \frac{\sqrt{\pi}}{2}\,\alpha\left(1-\theta_{\mathrm{thr}}\right)\mathrm{e}^{z_1^2}\,\mathrm{erfc}(z_1) - z_1\,\mathrm{e}^{-\alpha}\,, \\ \mathrm{e}^{\alpha}&\left(\theta_{\max}-\theta_{\mathrm{thr}}\right)\mathrm{e}^{z_2^2}\,\mathrm{erfc}(z_2) = \theta_{\mathrm{thr}}\,\mathrm{e}^{z_1^2}\,\mathrm{erfc}(z_1) \end{aligned} \tag{5.7}$$

which are obtained from equations (A.9) taking into account the definition (5.6). Thus, the concentration profile in the case of non-monotonous diffusion coefficient is characterized by the existence of a plateau where the concentration of adatoms does not depend on the spatial variable x. The length of the plateau $\ell_{\mathrm{p}} = 2\sqrt{\tau}\,(z_1 + z_2\,\mathrm{e}^{\alpha})$ increases with time. Such a behavior is shown in figure 6. The rate with which the length ℓ_{p} of the plateau increases is determined by the nonlinear parameter α and the threshold coverage θ_{thr}. We also carried out numerical simulations of equations (3.18) with the the step-like on-site energy $\mathscr{E}_n = \alpha\left\{1+\tanh\left[\kappa\left(\theta_n-\theta_{\mathrm{thr}}\right)\right]\right\}$ and, as it is seen from figure 7, our simple model (5.5) is in reasonable agreement with numerics. Note that the plateau in the concentration dependence develops only at the intermediate stage of the evolution. For large enough times, the concentration profile flattens, the effects of interatomic interactions become negligible and the profile evolves in accordance with the linear diffusion equation (see figure 7).

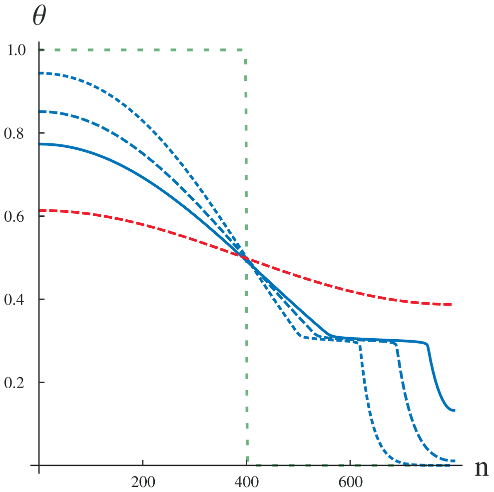

Figure 7. (Color online) Numerically obtained from equations (3.18) concentration profiles in the case of the step function energy dependence given by equation (5.4) with $\theta_{\mathrm{thr}} = 0.5$, $\alpha = 1$, $\kappa = 20$ for different time moments: $t = 0$ (dotted gray line), $t = 6000$ (dotted line), $t = 12000$ (dashed line), $t = 20000$ (solid line), $t = 40000$ (dashed, red, thick line).

It is worth noting that the diffusion of Dy adatoms absorbed by Mo(112) for the initial coverage $\theta(x,0) \approx 0.7H(-x)$ shows a very well pronounced plateau in the concentration profile dependence both on the spatial coordinate for different time moments and on the Boltzmann variable (see figures 7 and 8 in [11]). It means that according to our analytical considerations, the length of the plateau increases as $t^{1/2}$. This suggests that our simple analytical model may be a useful tool in analyzing the experimentally observed concentration behavior.

6. Conclusions and discussion

In this paper, we have investigated the role of interactions between adatoms in surface diffusion. The problem was considered analytically in the mean-field approach. By analyzing discrete nonlinear random walk equations and the corresponding nonlinear diffusion equations with an initial condition in the form of step-like concentration profile, we have found that the interactions between adatoms greatly effect the concentration profile development at on early and the intermediate stages of the process. In the case of low coverage, the interaction between adatoms makes the concentration profile asymmetric: it is shifted towards high concentration in the case of repulsive interactions and towards low concentration for attractive interactions. By calculating the magnitude of the shift, one can estimate the intensity of lateral interactions between adatoms. At the late stage of kinetics, the role of interatomic interactions becomes negligible. By studying the nonlinear random walk process which is characterized by a sharp maximum in the concentration dependence of the diffusivity, we have found that a well-pronounced plateau develops in the concentration profile. The length of the plateau increases in time as $t^{1/2}$. The coverage in the plateau θ_{thr} corresponds to the maximum of the diffusion coefficient which within the framework of our approach corresponds to a sharp decrease in the heat of adsorption as a function of coverage. The rate with which the length of the plateau increases with time is determined by an amount at which the adsorption heat drops at the threshold coverage θ_{thr}. All the above mentioned results were and can further be verified experimentally.

Acknowledgements

The authors acknowledge support from a Goal-oriented program of the National Academy of Sciences of Ukraine.

Appendix

The nonlinear diffusion equation (2.6) with the diffusion coefficient (5.5) and the initial condition (3.1) has a self-similar solution $\theta(x,\tau) \equiv \Theta(z)$, ($z = x/2\sqrt{\tau}$) which satisfies the equation

$$-2\,z\,\frac{\mathrm{d}\Theta}{\mathrm{d}z} = \frac{\mathrm{d}}{\mathrm{d}z}\left[D(\Theta)\,\frac{\mathrm{d}\Theta}{\mathrm{d}z}\right]. \tag{A.1}$$

The boundary conditions for equation (A.1) are

$$\begin{aligned} &\Theta(z) \to \Theta, \qquad \text{for} \qquad z \to -\infty\,, \\ &\Theta(z) \to 0, \qquad \text{for} \qquad z \to \infty\,. \end{aligned} \tag{A.2}$$

From equations (A.1) and (5.5) we see that the function

$$y(\Theta) = \int\limits_0^{\Theta} \mathrm{d}\Theta'\, z(\Theta')\,, \tag{A.3}$$

where $z(\Theta)$ is an inverse function with respect to $\Theta(z)$, satisfies the equation

$$-2\,\frac{\mathrm{d}^2 y}{\mathrm{d}\Theta^2} = D(\Theta)\,\frac{1}{y} \tag{A.4}$$

or equivalently, two equations

$$\begin{aligned} -2\frac{\mathrm{d}^2 y}{\mathrm{d}\Theta^2} &= \frac{1}{y}, \qquad \text{for} \qquad \Theta < \theta_{\mathrm{thr}}\,, \\ -2\frac{\mathrm{d}^2 y}{\mathrm{d}\Theta^2} &= \frac{1+b}{y}, \qquad \text{for} \qquad \Theta > \theta_{\mathrm{thr}} \end{aligned} \tag{A.5}$$

augmented by the jump condition

$$\left.\frac{\mathrm{d}y}{\mathrm{d}\Theta}\right|_{\Theta=\theta_{\mathrm{thr}}+0} - \left.\frac{\mathrm{d}y}{\mathrm{d}\Theta}\right|_{\Theta=\theta_{\mathrm{thr}}-0} = -\frac{a}{2\,y(\theta_{\mathrm{c}})}\,, \tag{A.6}$$

and the continuity condition

$$y(\theta_{\mathrm{thr}}+0) = y(\theta_{\mathrm{thr}}-0) = y(\theta_{\mathrm{c}})\,. \tag{A.7}$$

By integrating equations (A.5), we get

$$\begin{aligned} \frac{\mathrm{d}y}{\mathrm{d}\Theta} &= \sqrt{2z_1 + \ln\frac{y(\theta_{\mathrm{thr}})}{y}}, \qquad \text{for} \qquad \Theta < \theta_{\mathrm{thr}}\,, \\ -\frac{1}{\sqrt{1+b}}\frac{\mathrm{d}y}{\mathrm{d}\Theta} &= \sqrt{2\,z_2 + \ln\frac{y(\theta_{\mathrm{thr}})}{y}}, \qquad \text{for} \qquad \Theta > \theta_{\mathrm{thr}}\,, \end{aligned} \tag{A.8}$$

where the constants $y(\theta_{\mathrm{thr}})$, z_1 and z_2 satisfy the equations

$$\begin{aligned} \theta_{\mathrm{thr}} &= \frac{\sqrt{\pi}}{2}\frac{a}{z_1 + \sqrt{1+b}\,z_2}\,\mathrm{e}^{z_1^2}\,\mathrm{erfc}(z_1)\,, \\ \sqrt{1+b}\left(\theta_{\max} - \theta_{\mathrm{thr}}\right) &= \frac{\sqrt{\pi}}{2}\frac{a}{z_1 + \sqrt{1+b}\,z_2}\,\mathrm{e}^{z_2^2}\,\mathrm{erfc}(z_2), \\ y(\theta_{\mathrm{thr}}) &= \frac{a}{z_1 + \sqrt{1+b}\,z_2} \end{aligned} \tag{A.9}$$

which were obtained from the jump condition (A.6) and the continuity condition (A.7). Taking into account the definition (A.3), we eventually obtain from equations (A.5) that the concentration profile is determined by the following expressions

$$\begin{aligned} &\theta(z) = \theta_{\mathrm{thr}}\,\frac{\mathrm{erfc}(z)}{\mathrm{erfc}(z_1)} && \text{when} \;\; z \geqslant z_1\,, \\ &\theta(z) = \theta_{\mathrm{thr}} && \text{when} \;\; -\sqrt{1+b}\,z_2 \leqslant z \leqslant z_1\,, \\ &\theta(z) = \theta_{\max} - \left(\theta_{\max} - \theta_{\mathrm{thr}}\right)\frac{\mathrm{erfc}\left(-z/\sqrt{1+b}\right)}{\mathrm{erfc}(z_2)} && \text{when} \;\; z \leqslant -z_2\,\sqrt{1+b}\,. \end{aligned} \tag{A.10}$$

References

1. Gomer R., Rep. Prog. Phys., 1990, **53**, 917; doi:10.1088/0034-4885/53/7/002.
2. Naumovets A.G., Vedula A.S., Surf. Sci. Rep., 1985, **4**, 365; doi:10.1016/0167-5729(85)90007-X.
3. Gouyet J.F., Plapp M., Dietrich W., Maas P., Adv. Phys., 2003, **52**, 523; doi:10.1080/00018730310001615932.
4. Ala-Nissilla T., Ferrando R., Ying S.C., Adv. Phys., 2002, **51** 949; doi:10.1080/00018730110107902.
5. Naumovets A.G., Physica A, 2005, **357**, 189; doi:10.1016/j.physa.2005.06.027.
6. Antezak G., Ehrlich G., Surface Diffusion: Metals, Metal Atoms, and Clusters, Cambridge University Press, Cambridge, 2010.
7. Freimuth R.D., Lam L., Modeling Complex Phenomena, Springer, New York, 1992.
8. Gaididei Yu.B., J. Biol. Phys., 1993, **19**, 19; doi:10.1007/BF00700128.
9. Sheng-You Huang, Xian-Wu Zou, Wen-Bing Zhang, Zhun-Zhi Jin, Phys. Rev. Lett., 2002, **88**, 056102; doi:10.1103/PhysRevLett.88.056102.

10. Bowker M., King D.A., Surf. Sci., 1978, **72**, 208; doi:10.1016/0039-6028(78)90389-8.
11. Nikitin A.G., Spichak S.V., Vedula Yu.S., Naumovets A.G., J. Phys. D: Appl. Phys., 2009, **42**, 055301; doi:10.1088/0022-3727/42/5/055301.
12. Crank J., The Mathematics of Diffusion, Clarendon Press, Oxford, 1975.
13. Vedula Yu.S., Naumovets A.G., In: Surface Diffusion and Spreading, Geguzin Ya. (Ed.), Nauka, Moscow, 1969, 149–160 (in Russian).
14. Braun O.M., Medvedev V.K., Sov. Phys. Uspekhi, 1989, **32**, 328; doi:10.1070/PU1989v032n04ABEH002700.
15. Adamson A.W., Physical Chemistry of Surfaces (3rd ed.), Wiley, New York, 1976, Ch. XIV.
16. Loburets A.T., Naumovets A., Vedula Yu.S., In: Surface Diffusion. Atomistic and Collective Processes, Tringides M.C. (Ed.), Plenum, New York, 509–528.
17. It is worth noting that equation (5.2) is valid for $\theta < 1$ and the divergence $D(\theta)$ for $\theta \to 1$ is a model effect. It does not appear when the possibility of filling the second and next monolayers is taken into consideration.
18. Küntz M., Lavallée P., J. Phys. D: Appl. Phys., 2003, **36**, 1135; doi:10.1088/0022-3727/36/9/312.
19. Küntz M., Lavallée P., J. Phys. D: Appl. Phys., 2004, **37**, L5; doi:10.1088/0022-3727/37/1/L02.
20. Handbook of Mathematical Functions with Formulas, Graphs, and Mathematical Tables, Abramowitz M., Stegun I.A. (Eds.), Dover Publications, New York, 1972.
21. Butz R., Wagner H., Surf. Sci., 1977, **63**, 448; doi:10.1016/0039-6028(77)90358-2.
22. Smirnov A.A., Theory of Diffusion in Interstitial Alloys, Naukova Dumka, Kiev, 1982 (in Russian).
23. Zubarev D.N., Nonequilibrium Statistical Thermodynamics, Nauka, Moscow, 1971 (in Russian).
24. Chumak A.A., Tarasenko A.A., Surf. Sci., 1980, **91**, 694; doi:10.1016/0039-6028(80)90360-X.
25. Naumovets A.G., Contemp. Phys., 1989, **30**, 187; doi:10.1080/00107518908222596.
26. For a number of metal-on-metal systems a sharp D maximum is observed at submonolayer coverages corresponding to an initial stage of commensurate-incommensurate (C-I) phase transition [15, 27]. The transition starts with a local breaking of the commensurability, namely with formation of incommensurate walls which separate commensurate domains [28]. The domain walls can be considered as misfit dislocations in the commensurate phase and described as topological solitons [16]. Such objects were predicted and treated theoretically, and also detected experimentally by low-energy electron diffraction and scanning tunneling microscopy [29]. The solitons were shown to possess a high mobility and thus play a role of effective mass carriers in surface diffusion process. It is interesting to note that the highest diffusion rate is observed at the initial stages of C-I transition when the number of solitons is small. As their number grows, the diffusion rate decreases, so the coverage dependence of the diffusion coefficient is non-monotonous. This behaviour resembles the non-monotonous dependence of material strength on the concentration of dislocations: the strength increases when the dislocations are so numerous that they are pinning each other.
27. Masuda T., Barnes T.J., Hu P., King D.A., Surf. Sci., 1992, **276**, 122; doi:10.1016/0039-6028(92)90701-7.
28. Lyuksyutov I.F., Naumovets A.G., Pokrovsky V.L., Two-Dimensional Crystals, Academic Press, Boston, 1992.
29. Andryushechkin B.V., Eltsov K.N., Shevlyuga V.M., Surf. Sci., 2001, **472**, 80; doi:10.1016/S0039-6028(00)00926-2.

Вплив адатомної взаємодії на поверхневу дифузію

Ю.В. Гайдідей[1], В.М. Локтєв[1], А.Г. Наумовець[2], А.Г. Загородній[1]

[1] Інститут теоретичної фізики ім. М.М. Боголюбова НАН України,
вул. Метрологічна, 14 б, 03680 Київ, Україна

[2] Інститут фізики НАН України, просп. Науки, 46, 03680 Київ, Україна

Мотивовані недавніми дослідженнями Нікітіна та ін. [J. Phys. D: Appl. Phys., 2009, **49**, 055301], ми вивчаємо вплив міжатомних взаємодій на адатомну поверхневу дифузію. Використовуючи середньо-польовий підхід у проблемі випадкових блукань, ми виводимо нелінійне рівняння дифузії і аналізуємо його розв'язки. Результати нашого аналізу добре узгоджуються з прямими числовими симуляціями відповідної дискретної моделі. Показано, що, аналізуючи часову залежність профілів адатомної концентрації, можна оцінити тип і силу міжатомної взаємодії.

Ключові слова: *адатом, поверхня, нелінійна дифузія, числові симуляції*